Electronic Supplementary Information

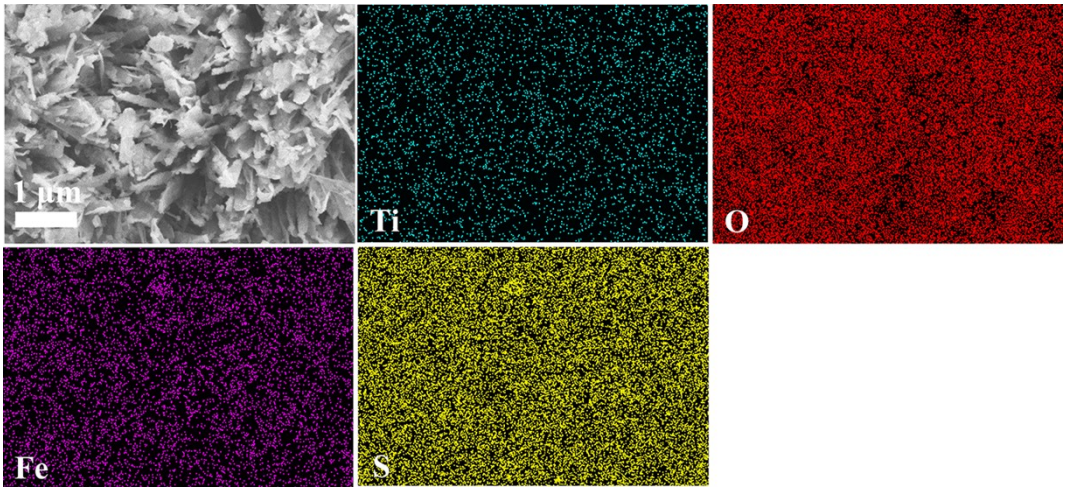

Fig. S1. SEM mapping images of FeS_2@TiO_2 heterostructure.

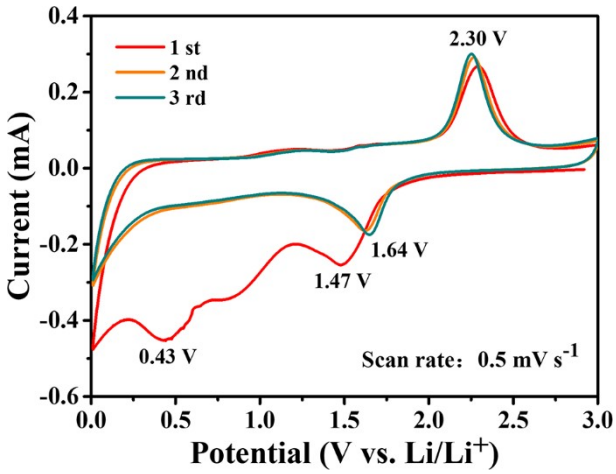

Fig. S2. CV curves for the initial three cycles of TiO_2 electrode at 0.5 mV s^{-1}.

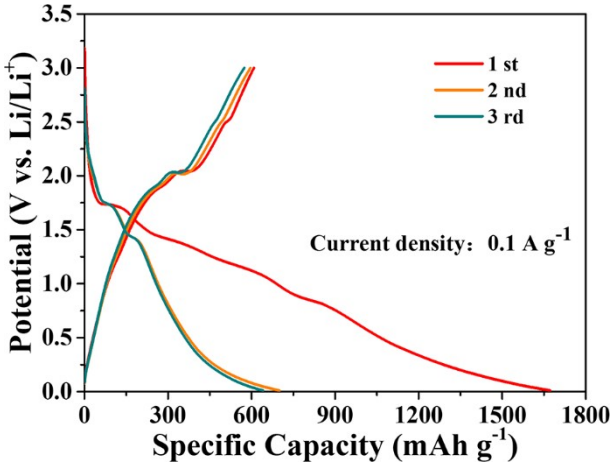

Fig. S3. Galvanostatic discharge-charge curves of FeS_2@TiO_2 heterostructure electrode at 0.1 A g^{-1}.

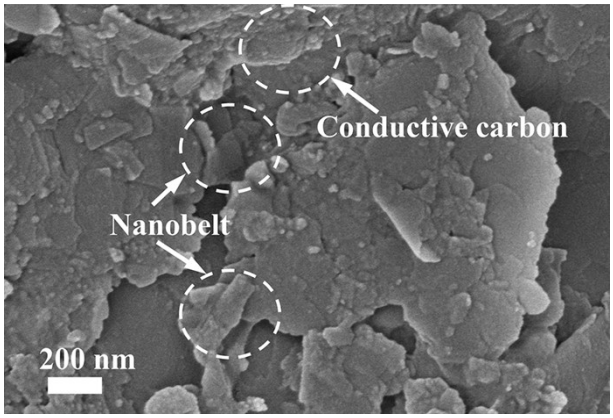

Fig. S4 SEM image of FeS_2@TiO_2 heterostructure after cycling.

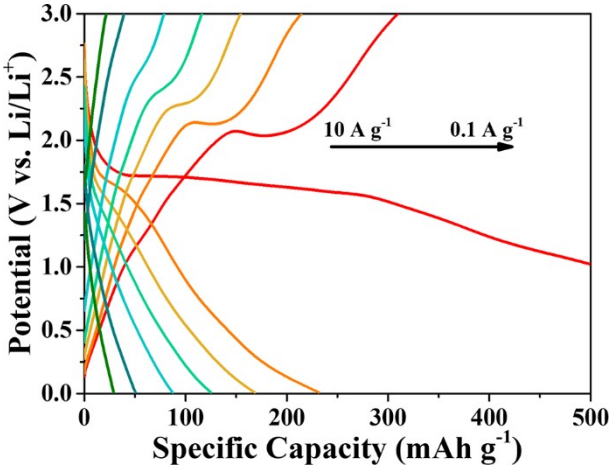

Fig. S5. Galvanostatic discharge-charge curves of TiO_2 electrode under various current densities

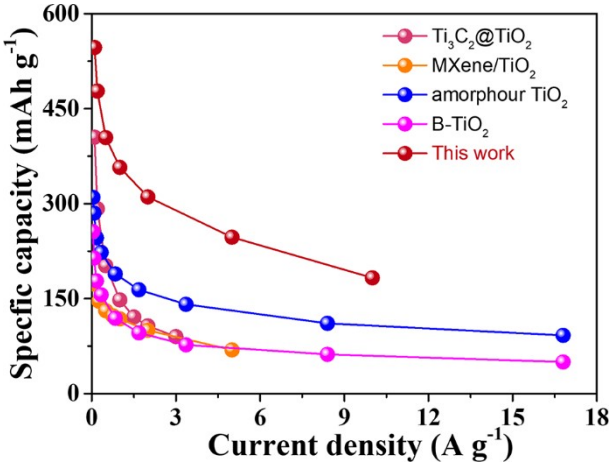

Fig. S6. Comparison on the rate performance between this work and other reported TiO_2-based anode.

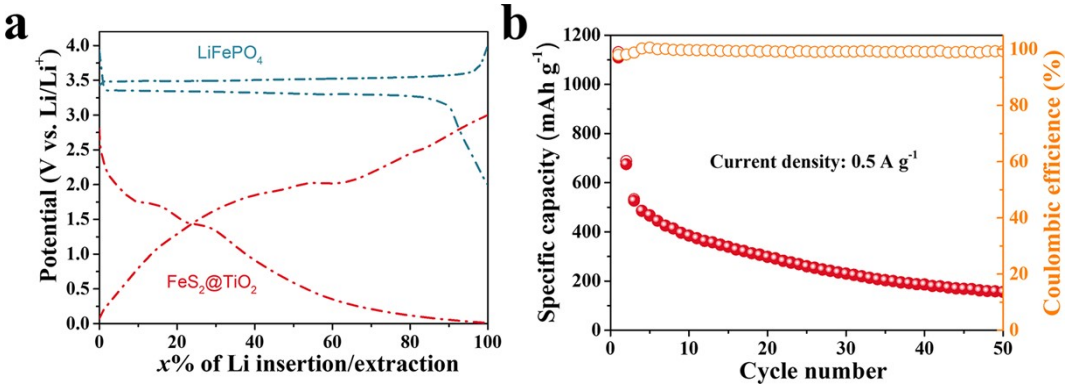

Fig. S7 (a) charge-discharge curves of FeS_2@TiO_2 and $LiFePO_4$ electrode. (b) Cycling performance of FeS_2@TiO_2||$LiFePO_4$ full cell.

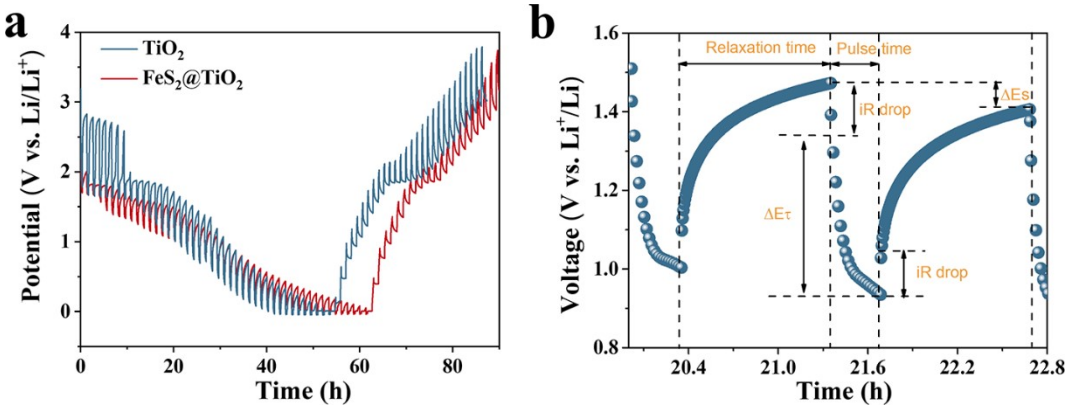

Fig. S8. (a) GITT profiles of TiO_2 and FeS_2@TiO_2. (b) Discharge profiles of FeS_2@TiO_2 electrode for a single GITT during discharge process.

Table S1 ICP analysis of FeS_2@TiO_2 heterojunction.

Sample	Fe (wt.%)	Ni (wt.%)
FeS_2@TiO_2	2.95	26.4

Table S2 Fitting results of EIS with the proposed equivalent circuit.

Materials	R_s **(Ω)**	R_{ct} **(Ω)**	**σ (Ω cm^2 s$^{-1/2}$)**
TiO_2	5.68	972.4	32.1
FeS_2@TiO_2	2.81	421.0	31.6